

Computational Prediction of Antibody Binding Sites on Tetracycline Antibiotics: Electrostatic Potentials and Average Local Ionization Energies on Molecular Surfaces

Pankaj Kulshrestha,[†] N. Sukumar,[‡] Jane S. Murray,^{*,§,||} Rossman F. Giese,[⊥] and Troy D. Wood[†]

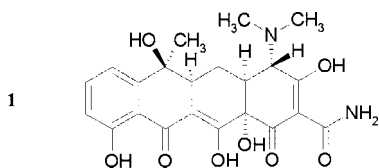
Department of Chemistry, University at Buffalo, The State University of New York, Buffalo, New York 14260, Center for Biotechnology and Interdisciplinary Studies, Rensselaer Polytechnic Institute, Troy, New York 12180, Department of Chemistry, University of New Orleans, New Orleans, Louisiana 70148, Department of Chemistry, Cleveland State University, Cleveland, Ohio 44115, and Department of Geology, University at Buffalo, The State University of New York, Buffalo, New York 14260

Received: October 8, 2008; Revised Manuscript Received: November 14, 2008

Enzyme linked immunosorbent assay (ELISA) was used for the analysis of tetracycline, chlortetracycline, oxytetracycline, and their transformed compounds in environmental water samples. The antibodies employed in ELISA showed high relative affinity for tetracycline, epitetracycline, chlortetracycline, and epichlortetracycline as compared to anhydrotetracycline, epianhydrotetracycline, and anhydrochlortetracycline. The specificity and crossreactivity of these antibodies are discussed in relation to the electrostatic potentials and average local ionization energies computed on the molecular surfaces of tetracycline antibiotics and their transformed compounds with an objective of identifying common features as well as differences that may be related to the experimentally observed variation in cross-reactivity values. The computations were performed at both the HF/STO-3G and HF/6-31+G* levels using the Gaussian 98 program. The results in this study are based upon molecular electrostatic potentials and local ionization energies computed on isodensity molecular surfaces. The surface electrostatic potentials are characterized in terms of a group of statistically defined quantities, which include the average deviation, the positive, negative, and total variances, positive and negative surface extrema, and a parameter indicating the degree of electrostatic balance.

Introduction

The tetracycline family of antibiotics, for which tetracycline (**1**) is the well-known parent compound, is commonly used in intensive animal agriculture systems as feed additives in animal feed, to treat infectious diseases and promote growth in food animals.



Widespread use of these antibiotics has led to the development of antibiotic-resistant microorganisms that are difficult to treat with existing antibiotics.^{1–5} The antibiotic dose varies from 1 to 100 mg/g of feed depending on the type and size of the animal. Most of the antibiotics added to animal feed are excreted in an unchanged form in urine or feces.⁶ These antibiotics may enter surface and groundwater through nonpoint source of pollution from sewage- and manure-applied agricultural fields

and have been shown to transform to structurally similar compounds under environmental conditions, forming epimers and anhydromers.^{7–10} In a study conducted under laboratory conditions, tetracycline anhydromers were found to be more toxic to soil microflora as compared to the parent tetracycline antibiotics.¹⁰ The United States Geological Survey (USGS) reported the presence of several antibiotics in 139 streams across 30 states in the USA.¹¹

Current chromatographic techniques, although able to achieve the required sensitivity, are time-consuming due to sample cleanup necessary and the relatively slow sample throughput achievable. Enzyme linked immunosorbent assay (ELISA) provides an alternative, specific, low-cost, and fast analytical methodology by taking advantage of the highly selective binding by antibodies.^{12,13}

The electrostatic potential $V(\mathbf{r})$ that is created in the space around the molecule by its nuclei and electrons can provide insight into molecular reactive behavior.^{14–16} It is defined by the following equation (eq 1), in which the molecule is treated as a collection of stationary point charges, the nuclei, that is surrounded by a continuous but static distribution of electrons.

$$V(\mathbf{r}) = \sum [Z_A / |\mathbf{R}_A - \mathbf{r}|] - \int [\rho(\mathbf{r}') / |\mathbf{r}' - \mathbf{r}|] \quad (1)$$

where Z_A is the charge on nucleus A that is located at \mathbf{R}_A , and $\rho(\mathbf{r})$ is the electronic density function of the molecule. The first term on the right side of eq 1 is the nuclear contribution and is therefore positive, whereas the second term is the electronic contribution to $V(\mathbf{r})$ and is negative.

The intermolecular forces that are involved in antigen–antibody interactions include hydrogen bonding, dispersion, induction,

* Corresponding author.

[†] Department of Chemistry, University at Buffalo, The State University of New York.

[‡] Center for Biotechnology and Interdisciplinary Studies, Rensselaer Polytechnic Institute.

[§] Department of Chemistry, University of New Orleans.

^{||} Department of Chemistry, Cleveland State University.

[⊥] Department of Geology, University at Buffalo, The State University of New York.

ionic bonding, hydrophobic interactions, and van der Waals interactions. While it is very useful to describe noncovalent interactions in terms of the types of forces that are involved, it has been pointed out in several studies that most of these are predominantly electrostatic in nature.^{17–21} The electrostatic potential of a system is a fundamental quantity since Poisson's equation connects it to the electronic density²² that in turn has been shown by Hohenberg and Kohn to be a determinant of a molecular system's properties.²³ Since a pioneering study by Scrocco and Tomasi,^{24–29} the electrostatic potential has been widely used to identify the molecular regions most susceptible to electrophilic and nucleophilic attack and for determining general molecular surface patterns of positive and negative potential that promote molecular interactions such as DNA binding sites on proteins and pharmaceutical binding sites on receptors crucial to elicit response.^{30,31}

The electrostatic potential computed on a surface of a molecule will have one or more local positive and negative extrema, $V_{S,\max}$ and $V_{S,\min}$; these are key site-specific quantities which can be related to hydrogen bond acidity and basicity, respectively.³² A suitable molecular surface is the electronic density contour of 0.001 au, suggested by Bader et al.³³ In several studies Politzer and Murray presented statistically defined quantities that characterize the features of the electrostatic potential on the molecular surface.^{14,34–36} These statistical quantities may make it possible to develop qualitative guidelines or even accurate quantitative analytical relationships for tetracycline-antibody binding. The following equations represent these quantities:

(A) Π is the average deviation of $V_S(\mathbf{r})$ and it is interpreted as a measure of the local polarity, or internal charge separation, that is present in a molecule.

$$\Pi = 1/t \sum_{i=1}^t |V_S(\mathbf{r}_i) - \bar{V}_S|$$

where t is the number of points on the surface grid and

$$\bar{V}_S = 1/t \left[\sum_{i=1}^t \bar{V}_S(\mathbf{r}_i) \right]$$

(B) σ_+^2 , σ_-^2 , and σ_{tot}^2 are the positive, negative, and total variances of $V_S(\mathbf{r})$, which reflect the range or variability of $V_S(\mathbf{r})$, emphasizing its surface extrema.

$$\sigma_+^2 = 1/n \sum_{i=1}^n [V_S^+(\mathbf{r}_i) - \bar{V}_S^+]^2$$

$$\sigma_-^2 = 1/m \sum_{i=1}^m [V_S^-(\mathbf{r}_i) - \bar{V}_S^-]^2$$

$$\sigma_{\text{tot}}^2 = \sigma_+^2 + \sigma_-^2$$

where n and m are the number of positive and negative points, respectively, and

$$\bar{V}_S^+ = 1/n \left[\sum_{i=1}^n V_S^+(\mathbf{r}_i) \right]$$

$$\bar{V}_S^- = 1/m \left[\sum_{i=1}^m V_S^-(\mathbf{r}_i) \right]$$

(C) ν indicates the degree of balance between the positive and negative surface potentials.

$$\nu = (\sigma_+^2 \sigma_-^2) / (\sigma_{\text{tot}}^2)^2$$

If $\sigma_+^2 = \sigma_-^2$, then ν achieves its maximum possible value of 0.25.

The ionization energy I of an atomic or molecular system is shown in various studies to be related to both the electronega-

tivity and polarizability.^{37–44} Since chemical reactivity is site-specific (local) rather than global, Sjöberg et al. introduced the average local ionization energy,⁴⁵ $\bar{I}(\mathbf{r})$, defined within the framework of Hartree–Fock (HF) theory that is presented by eq 2

$$\bar{I}(\mathbf{r}) = \sum_i (\rho_i(\mathbf{r}) |\epsilon_i|) / \rho(\mathbf{r}) \quad (2)$$

where $\rho_i(\mathbf{r})$ is the electronic density of the i th occupied atomic or molecular orbital at point \mathbf{r} , ϵ_i is the orbital energy, and $\rho(\mathbf{r})$ is the total electronic density function. $\bar{I}(\mathbf{r})$ is interpreted as the average energy needed to remove an electron from point \mathbf{r} in the space of an atom or molecule and therefore is suggested as a measure of local polarizability in molecules. To predict and interpret chemical behavior, $\bar{I}_S(\mathbf{r})$, i.e., the pattern of $\bar{I}(\mathbf{r})$ on the molecular surface, provides more useful information. The minima of $\bar{I}_S(\mathbf{r})$ ($\bar{I}_{S,\min}$) indicate the points on the molecular surface at which are found, on average, the least tightly bound, most reactive electrons. In a few studies of benzene derivatives, $\bar{I}_{S,\min}$ was found to correctly predict the ring-activating or -deactivating effects of substituents as well as their ortho/para- or meta-directing tendencies.^{45,46} This approach could be extended to tetracycline antibiotics to predict the effect of the functional groups on tetracycline molecular ring systems that could vary antibody recognition thereby resulting in different cross-reactivities.

The purpose of this study is to present surface electrostatic potentials and average local ionization energies of the tetracycline antibiotics and their environmentally relevant transformed compounds. Our aim is to discuss these computed properties in relation to the molecules' abilities to bind via noncovalent interactions to the tetracycline antibodies employed in ELISA, and to possibly explain the experimentally observed differences in their cross-reactivities.

Experimental Section

ELISA Method for Tetracycline Analysis. A commercially available ELISA method, developed for detection of tetracycline antibiotics in milk, honey, and meat was adapted to analyze manure-fertilized soil and wastewater samples.⁴⁷ The tetracycline ELISA (R-Biopharm GmbH, Darmstadt, Germany) used in this study consisted of a 96-well microtiter plate coated with tetracycline-bovine serum albumin conjugates. Samples or standards (50 μL /well) were added to the microwells followed by the addition of a solution of tetracycline antibodies (50 μL /well). The mixture was incubated at 25 °C for one hour and the wells were washed with phosphate buffered saline containing Tween 20 (PBS-Tween 20). A peroxidase conjugated secondary antibody solution (100 μL /well) against the tetracycline antibodies was added to each well and incubated at 25 °C for one hour. The wells were then washed with PBS-Tween 20 and the mixture (1:1 v/v, 100 μL /well) of substrate (urea peroxide) and chromogen (tetramethylbenzidine) were added and incubated at 25 °C for 15 min. Finally, sulfuric acid (1 M, 100 μL /well) was added into each well to stop the enzyme reaction. The absorbances were measured at 450 nm using a plate reader and the concentration of tetracycline present in the samples was calculated using a 4-parameter fit single plate transformation performed using KC4 software (Bio-Tek Instruments, Winooski, VT). This ELISA method could also detect epimers and anhydromers of parent tetracycline antibiotics.⁴⁷

Ab Initio Molecular Modeling. Due to the size of the tetracycline molecules, all optimized structures for tetracycline antibiotics and their transformed compounds were computed at

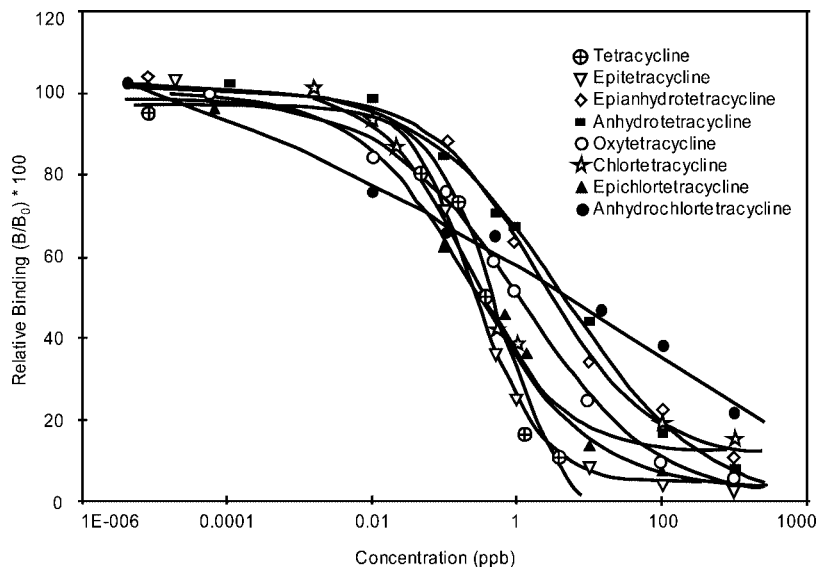


Figure 1. Cross-reactivity of ELISA for tetracycline antibiotics and their transformed compounds.

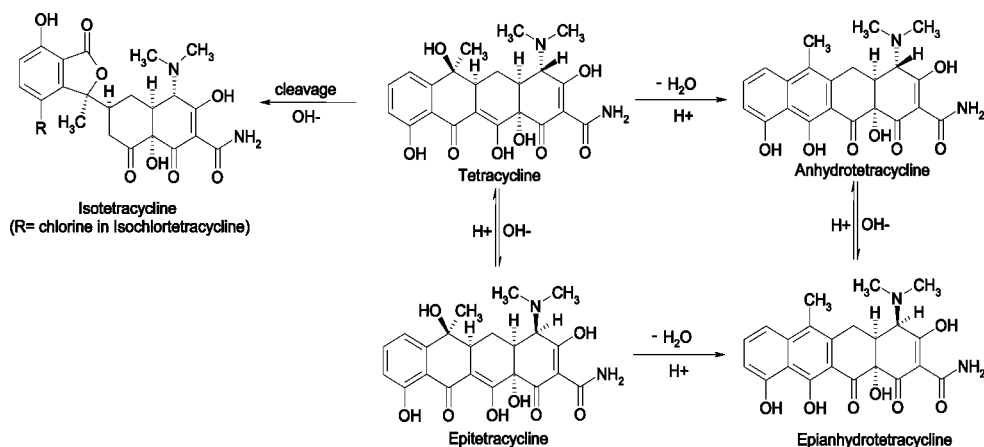


Figure 2. Degradation and transformation pathway of tetracycline antibiotics.

HF/STO-3G level using the Gaussian 98 system of programs.⁴⁸ This basis set has been used earlier in many computational studies for optimizing large systems, including pharmaceuticals.³¹

To see if surface properties computed with the STO-3G basis set could be viewed as reliable, single point computations using the STO-3G optimized geometries (to decrease computation time) were also done using a larger basis set, 6-31+G*, with an extended set of polarization and diffuse function. In comparing the results of these computations with those carried out at the HF/STO-3G level it was found that the surface properties showed the same relative trends. This has provided justification to proceed using our HF/STO-3G computations for investigating the variation in antibody cross-reactivities for our series of nine tetracycline compounds.

Using HF/STO-3G optimized geometries and wave functions, electrostatic potentials and average local ionization energies on molecular surfaces of all of the tetracycline compounds were computed and displayed using the Property-Encoded Surface Translator (PEST) software package version 3.2.⁴⁹ Plots for tetracycline, epitetracycline and anhydrotetracycline are shown in Figures 3–5, while plots for the other compounds can be found in the Supporting Information. A variety of statistical quantities in terms of these molecular surface properties were obtained using the HS95 (MOLSURF) program⁵⁰ that takes wave function input files generated from the Gaussian program;

these statistical quantities are tabulated in Table 2. The molecular surfaces were defined as corresponding to the 0.001 au contour of the electronic density.

Results and Discussion

Cross-Reactivities of Tetracycline-ELISA. The cross-reactivities of the antibodies toward other tetracycline antibiotics and their transformed compounds was determined using ELISA and is shown in Table 1 and Figure 1. The antibodies proved to be most sensitive toward epitetracycline, requiring only 0.27 ppb to result in a 50% reduction in the absorbance of the negative control (IC_{50}). Based on 80% inhibition (IC_{80}), the detection limit for epitetracycline is 0.02 ppb. The antibodies showed similar reactivities toward tetracycline ($IC_{50} = 0.47$), chlortetracycline ($IC_{50} = 0.35$), and epichlortetracycline ($IC_{50} = 0.30$). For oxytetracycline ($IC_{50} = 1.04$), the cross-reactivity was slightly lower as compared to tetracycline and chlortetracycline. The concentrations that cause 80% inhibition were 0.09 ppb, 0.05 ppb, and 0.04 ppb for oxytetracycline, tetracycline, and chlortetracycline, respectively. On the basis of this information, a detection limit of 0.09 ppb was set for tetracycline antibiotics.

Figure 2 shows the degradation and transformation pathway of parent tetracycline antibiotics. The tetracycline antibiotics can reversibly epimerize *in vitro* and *in vivo* at position C-4 to form corresponding epitetracycline, epichlortetracycline, and

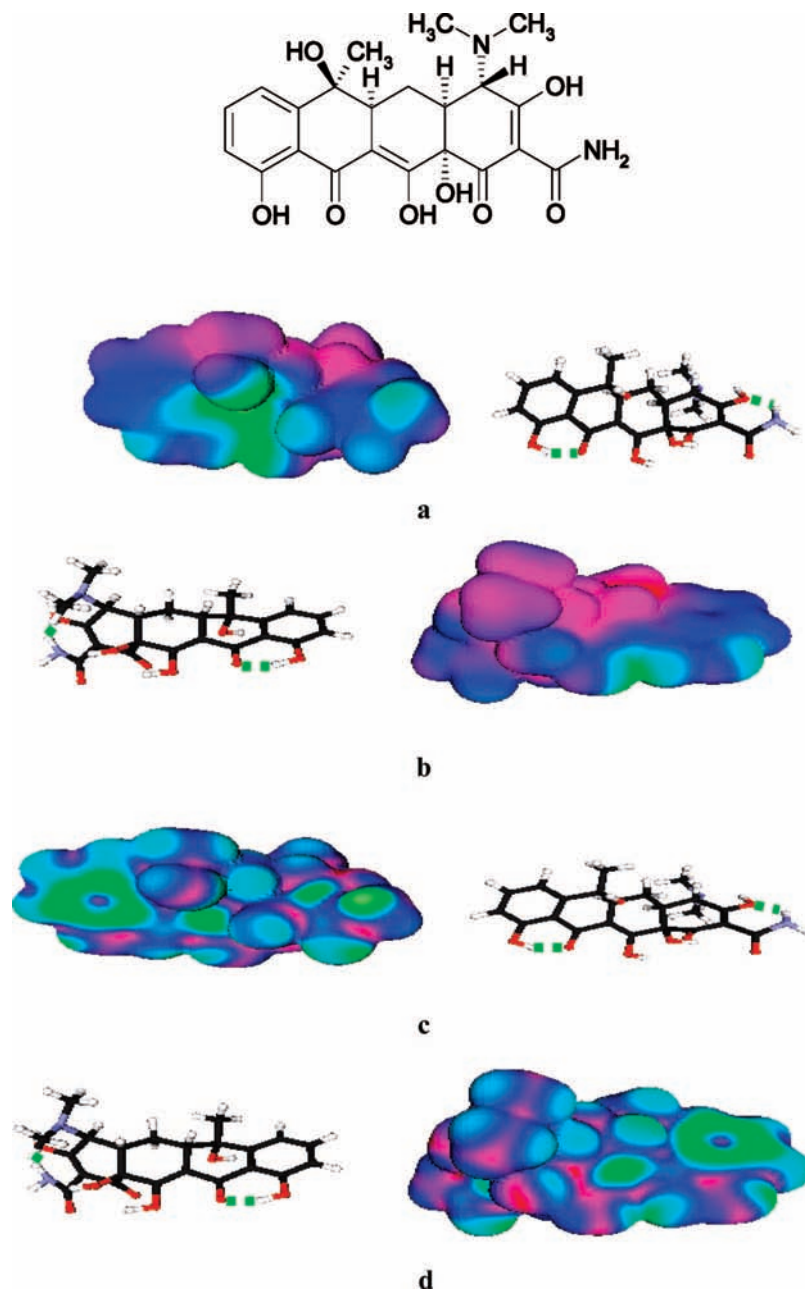


Figure 3. Optimized-geometry ball and stick models of tetracycline (**1**) showing its orientations are presented along with the electrostatic potential (views a and b) and the average local ionization energy (views c and d) mapped on its molecular surface; color ranges are given in the text.

epianhydrotetracycline (epimers)⁵¹ in the pH range from 2 to 7.⁵² Acidic environmental conditions also facilitate the loss of a water molecule by losing a hydroxyl group from position C-6 and a hydrogen from position C-5a, thus resulting in the formation of corresponding anhydrotetracycline, epianhydrotetracycline, and anhydrochlortetracycline (anhydromers) that have been reported to have several deleterious biological effects and are known as high-affinity ligands for the Tet repressor protein that up-regulates antibiotic efflux resistance mechanisms.^{53,54} The ELISA method used in this study was able to detect these transformed compounds with 80% inhibition observed at concentrations ranging from 0.18 to 0.24 ppb.

Under alkaline conditions the hydroxyl group at C-6 in chlortetracycline cleaves readily to form an isobenzofuran ring and thus transforms into isochlortetracycline.⁵⁵ One study showed that isochlortetracycline had no toxicity to both the tetracycline resistant and environmentally relevant soil/sludge

bacteria.^{55,56} Unavailability of positions C-11 and C-12 in isochlortetracycline for complexation with divalent and trivalent ions was considered to be the reason for its loss in potency relative to chlortetracycline and its other byproducts. Isochlortetracycline was not detectable by the ELISA method. In our previous study, ELISA could be used effectively to determine total tetracycline antibiotics and their toxic transformed byproduct in the environmental samples.⁴⁷

Explanation of Differences in Antibody Cross-Reactivities Observed in Tetracycline-ELISA Using Molecular Modeling.

Optimized-geometry ball and stick models of the tetracycline compounds are presented along with electrostatic potential (views a and b) and average local ionization energy (views c and d) mapped on electron density molecular surfaces as shown in Figures 3–11. The electrostatic potential in kcal/mol is represented by magenta (more positive than 18), red (between 18 and 10), orange (between 10 and 0), green (between 0 and

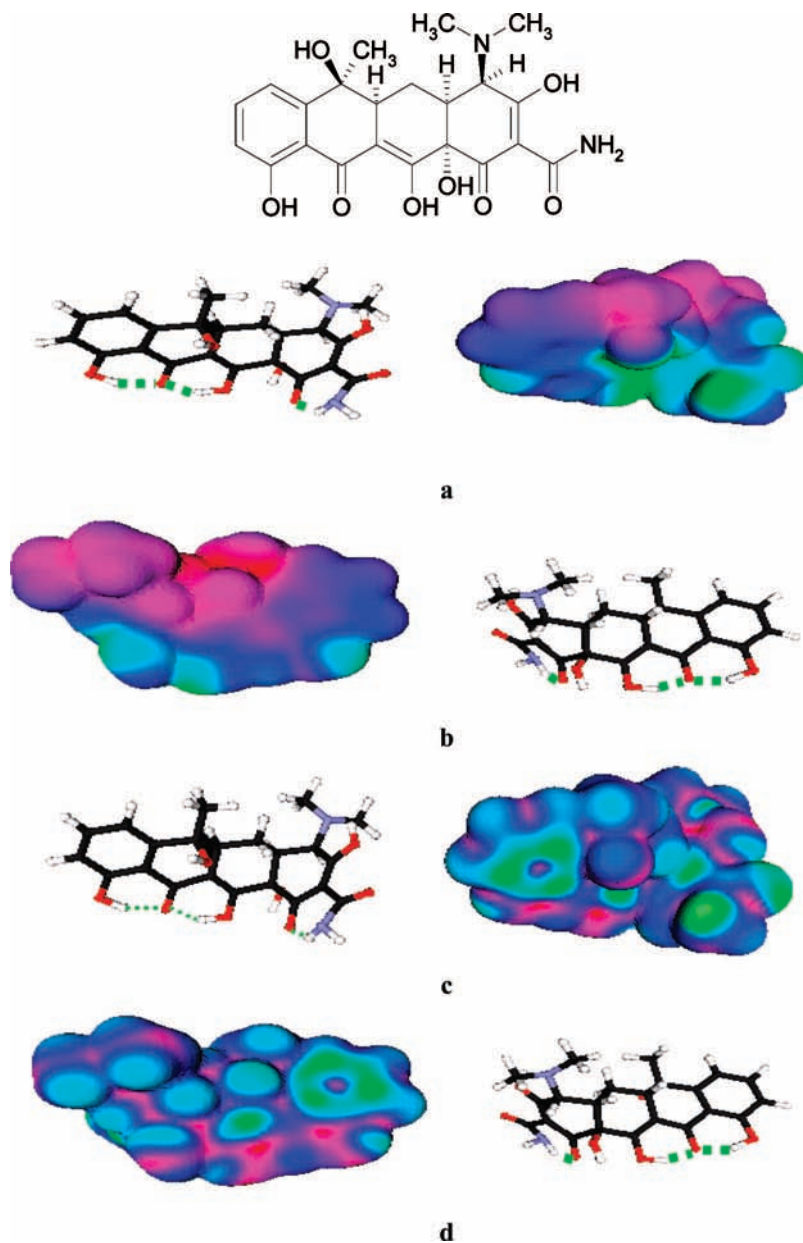


Figure 4. Optimized-geometry ball and stick models of epitetracycline (**2**) showing its orientations are presented along with the electrostatic potential (views a and b) and the average local ionization energy (views c and d) mapped on its molecular surface; color ranges are given in the text.

– 20), and blue (more negative than – 20). The ionization energy in eV is represented by blue (less than 12.5), green (between 12.5 and 14.2), orange (between 14.2 and 15.8), red (between 15.8 and 16.6), and magenta (greater than 16.6). The positive areas of the electrostatic potential maps are repulsive to a proton and negative areas are attractive to a proton. Table 2 shows the statistical quantities that adequately describe and quantitatively characterize the above-mentioned molecular surface properties for tetracycline compounds that are labeled for purposes of identification as tetracycline (**1**), epitetracycline (**2**), anhydrotetracycline (**3**), epianhydrotetracycline (**4**), chlortetracycline (**5**), epichlortetracycline (**6**), anhydrochlortetracycline (**7**), isochlortetracycline (**8**) and oxytetracycline (**9**).

Molecular Surface Electrostatic Potentials. Since the amine nitrogen in the ring A of tetracycline is conjugated to the bovine serum albumin protein in each microwell of the ELISA plate, the tetracycline antibody would bind to the lower region of these compounds, its affinity depending on how strong the noncovalent

interactions are between the tetracycline compounds and the antibody. It is clear from Figures 35 views a and b (Figures 6–11 views a and b in the Supporting Information) that the bottom edge of each tetracycline compound has a strong stretch of negative potential (shown in blue and green) that is associated with the amide nitrogen and the three hydroxyl and carbonyl oxygens that are positioned along the lower portion of the molecule. The negative region associated with the amide nitrogen lone pair is seen in view a of each figure since the lone pair points to only one side of each molecule.

Strong hydrogen bonds in the range 1.5–1.6 Å form an integral part of the lower skeleton of all tetracycline compounds. It is clearly seen that one of the amide hydrogens participates in intramolecular hydrogen bonding with hydroxyl of ring A of all compounds except in epitetracycline and epichlortetracycline where this amide hydrogen intramolecularly bonds with carbonyl of ring A. The carbonyl oxygen of ring C in tetracycline, chlortetracycline, and oxytetracycline is involved

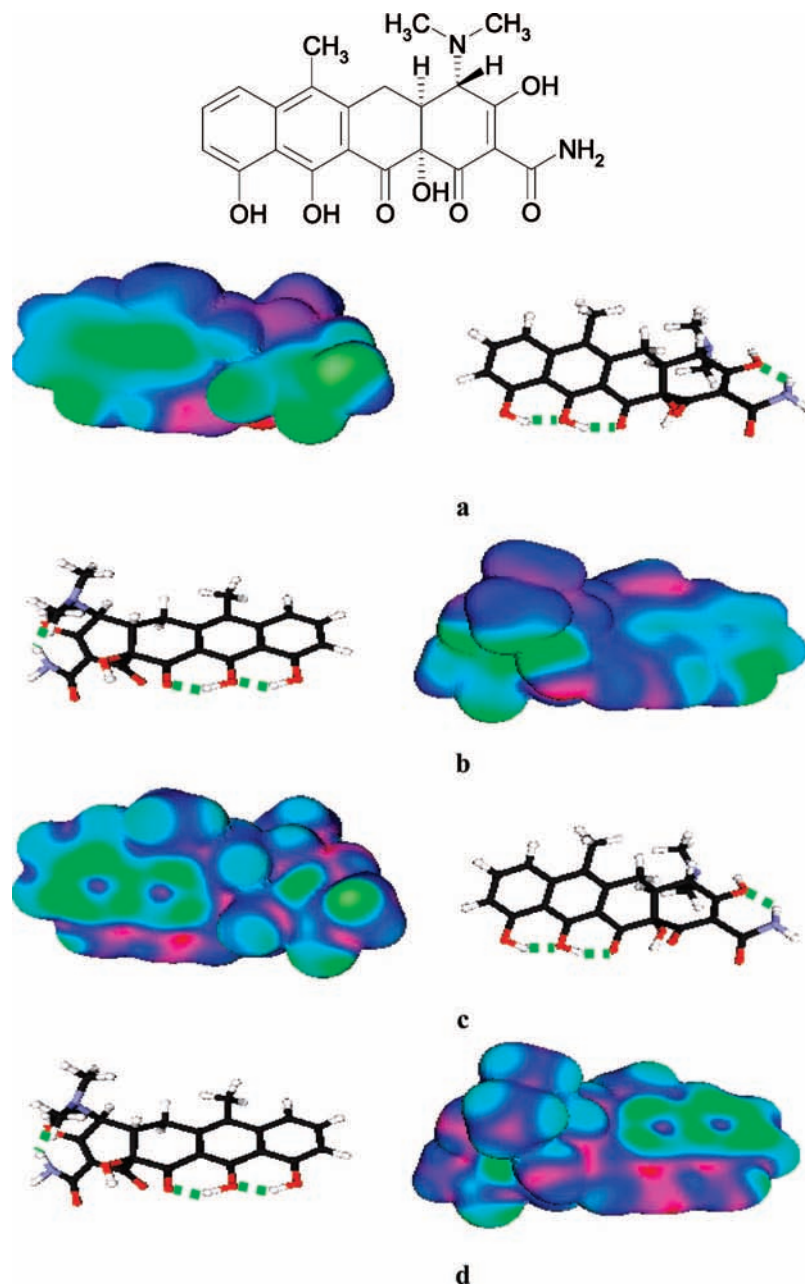


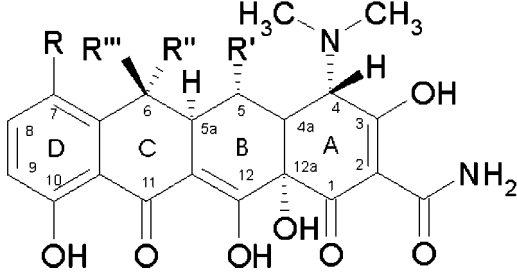
Figure 5. Optimized-geometry ball and stick models of anhydrotetracycline (**3**) showing its orientations are presented along with the electrostatic potential (views a and b) and the average local ionization energy (views c and d) mapped on its molecular surface; color ranges are given in the text.

in intramolecular hydrogen bonding with the neighboring hydroxyl hydrogen of ring D. Whereas in epitetracycline and epichlortetracycline, intramolecular hydrogen bonds are visible between the hydroxyl hydrogen on the lower portions of rings B and D and the carbonyl oxygen of ring C, in anhydromers, the hydroxyl hydrogen of ring D hydrogen bonds with hydroxyl oxygen of ring C and hydroxyl hydrogen of ring C hydrogen bonds with carbonyl oxygen of ring B. These interactions have somewhat neutralizing effects on the normally strong negative potential that is associated with carbonyl oxygen.

From Figures 35, view a and b (Figures 6–11, views a and b in the Supporting Information), it can be seen that the negative potentials associated with the hydrogen bonded functional groups are green rather than blue in color, providing evidence of their involvement in intramolecular hydrogen bonding. Such weakening of a typically strong negative potential due to intramolecular or intermolecular hydrogen bonding has been

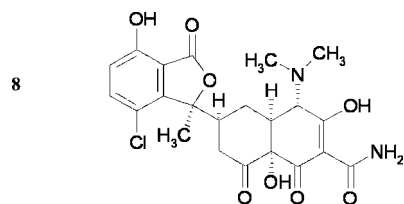
observed in many research studies and is characteristic of an interaction that reduces local polarity.^{57–59} It should be kept in mind, however, that other factors, such as strong electron-attracting groups, can diminish the strengths (magnitudes) of both positive and negative regions of potential.^{32,34}

The hydrogen bonding interactions that result in reducing the negative potential in the vicinity of hydrogen bonded functional groups on the surface of tetracycline molecules could influence the antibody cross-reactivities. This is further supported quantitatively from $V_{S,\min}$ and $V_{S,\max}$ values shown in Table 2. It is notable that $V_{S,\min}$ values of the carbonyl oxygens on ring C in tetracycline, chlortetracycline, oxytetracycline, epitetracycline, and epichlortetracycline and of the carbonyl oxygens on ring B in anhydromers are less negative than those of the carbonyl oxygens on ring A in all these molecules, suggesting involvement of the carbonyl oxygen on rings B and C in hydrogen bonding. The ground-state structure of isochlortetracycline (**8**)

TABLE 1: Cross-Reactivities of the Antibodies toward Tetracycline Antibiotics and Their Transformed Compounds Determined Using ELISA


antibiotic or transformed product	R'	R''	R'''	R	IC ₅₀ (ppb)	IC ₈₀ (ppb)
tetracycline, 1	H	CH ₃	OH	H	0.47	0.05
epitetracycline, 2	H	CH ₃	OH	H	0.27	0.02
anhydrotetracycline, 3	H	CH ₃		H	4.50	0.22
epianhydrotetracycline, 4	H	CH ₃		H	2.99	0.24
chlortetracycline, 5	H	CH ₃	OH	Cl	0.35	0.04
epichlortetracycline, 6	H	CH ₃	OH	Cl	0.30	0.03
anhydrochlortetracycline, 7	H	CH ₃		Cl	4.48	0.18
oxytetracycline, 9	OH	CH ₃	OH	H	1.04	0.09

is such that carbonyl oxygens are not involved in hydrogen bonding; this is reflected in the insignificant differences in the $V_{S,\min}$ values of the carbonyl oxygens on rings C and A of this molecule as compared to those of the other molecules.



Since the carbonyl oxygens on ring C are hydrogen bonded to hydrogens of the hydroxyl groups on rings B and D in epitetracycline and epichlortetracycline, significantly less negative $V_{S,\min}$ values are observed, compared to this carbonyl oxygen in any other tetracycline compounds. Moreover, less negative $V_{S,\min}$ values of the hydroxyl oxygens on ring A in all of the molecules except epitetracycline and epichlortetracycline suggests that this oxygen intramolecularly bonds to one of the neighboring amide hydrogens (the one with the smaller $V_{S,\max}$ value). In contrast, the hydroxyl oxygens on ring A of epitetracycline and epichlortetracycline have $V_{S,\min}$ values of around -60 kcal/mol, suggesting a lack of participation in hydrogen bonding. Also, in the anhydromers, less negative $V_{S,\min}$ values of the carbonyl oxygens on ring B and the hydroxyl oxygens on rings C and D suggest that they might be involved in hydrogen bonding interactions with hydroxyl hydrogens on rings C and D.

The anhydromers do not chemically or conformationally mimic the structures of their parent tetracycline compounds. A hydroxyl on ring B and a carbonyl on ring C in the parent compound are replaced by a carbonyl on ring B and a hydroxyl on ring C respectively in the corresponding anhydromers. In addition to the formation of strong intramolecular hydrogen bonds between the hydroxyl and carbonyl functional groups of rings B, C, and D in anhydromers as discussed previously, loss of a water molecule due to losing a hydroxyl on carbon number 6 of ring C and a hydrogen between rings B and C results in overall weakening of the negative electrostatic potential as observed in Figures 5, 6 (Supporting Information), and 9

(Supporting Information) and views a and b from the green and magenta areas on their molecular surface. As a consequence, loss in binding contacts in anhydromers results in a 10-fold decrease in antibody cross-reactivity as compared to the corresponding parent tetracyclines (Table 1). This also shows that the presence of a hydroxyl group on carbon number 6 of ring C is a significant factor favoring binding to the antibody.

In general, a positive potential is observed in Figures 3–5 views a and b (Figures 6–11 views a and b in the Supporting Information) along the top portion of all tetracycline molecules with the exception of a small area of negative potential shown in Figures 3, 4, 7 (Supporting Information), 8 (Supporting Information), and 11 (Supporting Information) view a, associated with the hydroxyl oxygen on ring C in tetracycline, epitetracycline, chlortetracycline, epichlortetracycline, and oxytetracycline. It is interesting to note that the hydroxyl group bonded to the top portion of ring B in oxytetracycline does not produce a strong negative potential. This hydroxyl group may create sterically hindered access to this region of the molecule (Table 2), possibly contributing to the 2-fold decrease in the affinity of the antibody toward oxytetracycline as compared to tetracycline and chlortetracycline (Table 1).

Only view a of the epimers in Figures 4, 6 (Supporting Information), and 8 (Supporting Information) show the negative region associated with the amine nitrogen lone pair of the ring A. This epimer configuration together with the neighboring methyl groups allows the lone pair of electrons of the amine nitrogens to point to the side of the molecule where the long stretch of negative potential is encountered by the antibody. This helps to explain the antibody's greater cross-reactivity toward epimers as compared to their parent compounds. The higher antibody affinities of the epimers may result from the fact that their amine nitrogens actually have negative (though weak) regions of electrostatic potential (Table 2), while those of the other molecules do not.

Another interesting feature associated with the surface potentials can be seen in Figures 3, 4, 5, 6 (Supporting Information), and 11 (Supporting Information), views a and b; these figures show the presence of a negative region (shown in blue-green) associated with ring D of tetracycline, epitetracycline, anhydrotetracycline, epianhydrotetracycline, and oxytetracycline. This type of negative region is attributed to the π electrons of an aromatic ring.³⁴ However, the presence of an

TABLE 2: Descriptors of Molecular Surface Properties of Tetracycline Compounds (Index Numbers Represent Tetracycline Molecules and Are Given in the Text)

molecule	surface area (Å ²)	Π (kcal/mol)	σ_+^2	σ_-^2 (kcal/mol) ²	σ_{tot}^2	ν	V_s , max (kcal/mol)	V_s , min (kcal/mol)	I_s ,min (eV)	log K_{ow}
1	398.3	16.3	66.8	202.2	268.9	0.19	H _{hydroxyl,ringA} : 31.9 H _{hydroxyl,ringC} : 16.9 H _{hydroxyl,ringD} : 13.6 H _{amide,ringA} : 22.1 H _{amide,ringA} : 18.2	O _{amide,ring A} : -43.1 N _{amide,ring A} : -41.0 O _{carbonyl,ring A} : -41.2 O _{hydroxyl,ring B} : -45.4 O _{hydroxyl,ring D} : -35.0 O _{hydroxyl,ring C} : -41.8 O _{carbonyl,ring C} : -17.3 O _{hydroxyl,ring A} : -6.9 O _{hydroxyl,ringA-B} : -59.9 N _{amine,ring A} : 4.39	N _{amide, ring A} : 12.1 C _{ring A-attached to amide} : 13.4 C _{ring D-para} : 13.4 C _{ring D-ortho} : 13.5 O _{amide, ring A} : 14.5	-3.4
2	397.5	13.5	37.8	212.2	250.1	0.13	H _{hydroxyl,ringA} : 20.3 H _{hydroxyl,ringC} : 15.8 H _{hydroxyl,ringD} : 21.0 H _{hydroxyl,ringB} : 23.1 H _{amide,ringA} : 13.9 H _{amide,ring A} : 8.1	O _{amide,ring A} : -61.9 N _{amide,ring A} : -48.3 O _{carbonyl,ring A} : -38.4 O _{hydroxyl,ring B} : -37.2 O _{hydroxyl,ring D} : -37.7 O _{hydroxyl,ring C} : -34.2 O _{carbonyl,ring C} : -8.1 O _{hydroxyl,ring A} : -62.0 O _{hydroxyl,ringA-B} : -11.5 N _{amine,ring A} : -5.35	N _{amide, ring A} : 11.6 C _{ring A-attached to amide} : 13.8 C _{ring D-para} : 13.8 C _{ring D-ortho} : 13.8 O _{amide ring A} : 13.9	-2.9
3	387.7	12.8	53.9	174.0	238.3	0.18	H _{hydroxyl,ringA} : 27.5 H _{hydroxyl,ringC} : 27.6 H _{hydroxyl,ringD} : 25.8 H _{amide,ringA} : 18.5 H _{amide,ringA} : 13.9	O _{amide,ring A} : -46.4 N _{amide,ring A} : -43.5 O _{carbonyl,ring A} : -42.2 O _{carbonyl,ring B} : -29.9 O _{hydroxyl,ring D} : -19.2 O _{hydroxyl,ring C} : -15.4 O _{hydroxyl,ring A} : -12.8 O _{hydroxyl,ringA-B} : -10.8 N _{amine,ring A} : 1.0	N _{amide, ring A} : 11.9 C _{ring A-attached to amide} : 13.2 C _{ring D-para} : 13.3 C _{ring D-ortho} : 13.7 O _{amide, ring A} : 14.2	2.2
4	387.5	12.7	49.3	189.0	227.9	0.16	H _{hydroxyl,ringA} : 29.1 H _{hydroxyl,ringC} : 26.9 H _{hydroxyl,ringD} : 22.8 H _{amide,ringA} : 18.4 H _{amide,ringA} : 14.3	O _{amide,ring A} : -53.9 N _{amide,ring A} : -41.9 O _{carbonyl,ring A} : -42.5 O _{carbonyl,ring B} : -27.2 O _{hydroxyl,ring D} : -19.9 O _{hydroxyl,ring C} : -17.2 O _{hydroxyl,ring A} : -14.3 O _{hydroxyl,ringA-B} : -11.2 N _{amine,ring A} : -1.25	N _{amide, ring A} : 11.9 C _{ring A-attached to amide} : 13.2 C _{ring D-para} : 13.7 C _{ring D-ortho} : 13.9 O _{amide, ring A} : 14.3	1.8
5	410.5	15.1	76.0	159.8	235.8	0.22	H _{hydroxyl,ringA} : 32.1 H _{hydroxyl,ringC} : 13.9 H _{hydroxyl,ringD} : 16.0 H _{amide,ringA} : 22.3 H _{amide,ringA} : 18.3 C _{11,ringD} : 21.8 C _{12,ringD} : 25.7	O _{amide,ring A} : -42.4 N _{amide,ring A} : -41.3 O _{carbonyl,ring A} : -40.1 O _{hydroxyl,ring B} : -40.0 O _{hydroxyl,ring D} : -36.6 O _{hydroxyl,ring C} : -27.4 C _{11,ringD} : -18.8 C _{12,ringD} : -15.2 O _{hydroxyl,ring A} : -6.9 O _{hydroxyl,ringA-B} : -49.9 N _{aminering A} : 4.61	N _{amide, ring A} : 12.2 C _{ring A-attached to amide} : 13.8 C _{ring D-para} : 14.3 C _{ring D-ortho} : 14.3 O _{amide, ring A} : 14.5	-1.6
6	409.4	13.4	41.2	175.6	216.8	0.15	H _{hydroxyl,ringA} : 21.2 H _{hydroxyl,ringC} : 14.6 H _{hydroxyl,ringB} : 24.9 H _{hydroxyl,ringD} : 23.7 H _{amide,ringA} : 15.2 H _{amide,ring A} : 9.8 C _{11,ringD} : 25.0 C _{12,ringD} : 25.5	O _{amide,ring A} : -60.7 N _{amide,ring A} : -46.1 O _{carbonyl,ring A} : -36.2 O _{hydroxyl,ring B} : -32.9 O _{hydroxyl,ring D} : -36.1 O _{hydroxyl,ring C} : -30.2 C _{11,ringD} : -15.7 C _{12,ringD} : -6.8 O _{hydroxyl,ring A} : -60.5 O _{hydroxyl,ringA-B} : -8.1 N _{amide,ring A} : -4.41	N _{amide, ring A} : 11.7 C _{ring A-attached to amide} : 14.3 C _{ring D-para} : 14.4 C _{ring D-ortho} : 14.5 O _{amide, ring A} : 13.8	-1.4
7	400.8	12.5	62.4	143.5	205.8	0.21	H _{hydroxyl,ringA} : 28.6 H _{hydroxyl,ringC} : 26.9 H _{hydroxyl,ringD} : 25.6 H _{amide,ringA} : 19.7 H _{amide,ringA} : 15.1 C _{11,ringD} : 22.7 C _{12,ringD} : 32.4	O _{amide,ring A} : -44.5 N _{amide,ring A} : -42.3 O _{carbonyl,ring A} : -40.3 O _{carbonyl,ring B} : -28.7 C _{11,ringD} : -20.5 O _{hydroxyl,ring D} : -18.3 O _{hydroxyl,ring C} : -12.5 O _{hydroxyl,ring A} : -11.5	N _{amide, ring A} : 12.00 C _{ring A-attached to amide} : 13.7 C _{ring D-para} : 14.3 C _{ring D-ortho} : 14.4 O _{amide, ring A} : 14.3	1.8

TABLE 2: Continued

molecule	surface area (Å ²)	Π (kcal/mol)	σ ₊ ²	σ ₋ ² (kcal/mol) ²	σ _{tot} ²	ν	V _s , max (kcal/mol)	V _s , min (kcal/mol)	I _{s,min} (eV)	log K _{ow}								
8	416.5	17.5	67.7	252.0	319.6	0.17	H _{hydroxyl,ringA} : 23.9 H _{amide,ringA} : 13.9 H _{amide,ringA} : 9.1 C _{11,ringD} : 27.2 C _{12,ringD} : 31.4	O _{hydroxyl,ring A-B} : -8.5 N _{amide,ring A} : 2.13 O _{amide,ring A} : -50.5 N _{amide,ring A} : -49.7 O _{carbonyl,ring A} : -51.5 O _{carbonyl,ring B} : -39.6 O _{hydroxyl,ring D} : -35.3 O _{carbonyl,ring C} : -43.6 C _{17,ring} : -10.9 O _{hydroxyl,ring A} : -12.8 O _{hydroxyl,ring A-B} : -17.7 N _{amide,ring A} : 8.43 O _{amide,ring A} : -44.7 N _{amide,ring A} : -42.0 O _{carbonyl,ring A} : -49.2 O _{hydroxyl,ring B} : -33.9 O _{hydroxyl,ring D} : -32.2 O _{hydroxyl,ring C} : -31.8 O _{carbonyl,ring C} : -15.3 O _{hydroxyl,ring A} : -9.8 O _{hydroxyl,ring A-B} : -42.1 O _{hydroxyl,ring B,above} : 17.7 N _{amide,ringA} : 11.45	N _{amide, ring A} : 11.6 C _{ring A-attached to amide} : 13.2 C _{ring D-para} : 16.9 C _{ring D-ortho} : 16.8 O _{amide, ring A} : 15.1	-3.6								
								9	395.9		13.4	58.2	240.8	0.13	H _{hydroxyl,ringA} : 28.4 H _{hydroxyl,ringC} : 15.1 H _{hydroxyl,ringD} : 21.0 H _{hydroxyl,ringB} : 25.7 H _{amide,ringA} : 19.8 H _{amide,ringA} : 15.2	O _{amide,ring A} : -44.7 N _{amide,ring A} : -42.0 O _{carbonyl,ring A} : -49.2 O _{hydroxyl,ring B} : -33.9 O _{hydroxyl,ring D} : -32.2 O _{hydroxyl,ring C} : -31.8 O _{carbonyl,ring C} : -15.3 O _{hydroxyl,ring A} : -9.8 O _{hydroxyl,ring A-B} : -42.1 O _{hydroxyl,ring B,above} : 17.7 N _{amide,ringA} : 11.45	N _{amide, ring A} : 12.0 C _{ring A-attached to amide} : 13.6 C _{ring D-para} : 13.6 C _{ring D-ortho} : 14.4	-1.1

electron-withdrawing substituent such as the chlorine on ring D in chlortetracycline, epichlortetracycline, anhydrochlortetracycline, and isochlortetracycline acts to eliminate this characteristic negative region. The absence of a negative potential (shown in magenta) associated with ring D in these chloro derivatives can be seen in Figures 7 (Supporting Information), 8 (Supporting Information), and 9 (Supporting Information), views a and b. This has been observed in many aromatic systems.³⁴ Even though chlorine attracts considerable charge, its large charge capacity and size results in an electrostatic potential that is only weakly negative, as is shown by green near the chlorine atoms in Figures 7 (Supporting Information), 8 (Supporting Information), and 9 (Supporting Information), views a and b.

The member compounds of the pairs tetracycline-chlortetracycline, epitetracycline-epichlortetracycline, and anhydrotetracycline-anhydrochlortetracycline differ only because of the absence or presence of a chloro substituent on ring D. Although the chlorines affect the potential above and below ring D, the mimicry of other, perhaps more significant, regions of the surface electrostatic potentials in these pairs presumably explains the almost equal relative affinities of the antibody to these pairs of tetracycline compounds, as shown in Table 1.

Isochlortetracycline (**8**), shown earlier, consists of an isobenzofuran ring in its chemical structure. The difference from parent chlortetracycline is also notable from Figure 10 (Supporting Information) in the electrostatic potential mapped on electron density surface of isochlortetracycline. Isochlortetracycline has the biggest surface area of all tetracycline compounds. The antibody does not show an affinity to isochlortetracycline at all, most probably due to its unique chemical structure, conformation and molecular surface properties. This isomer of chlortetracycline lacks the characteristic rigid four-fused-ring backbone seen in other members of the tetracycline family of drugs.

Statistical Quantities Derived from Surface Electrostatic Potentials. A detailed listing of the statistical quantities such as Π, σ₊², σ₋², σ_{tot}², and ν that describe and compare surface electrostatic potential for all tetracycline compounds is given

in Table 2. As explained previously Π is an average deviation of V_s(r) and is a measure of the local polarity, or internal charge separation present in all molecules. The computed Π values, in kcal/mol, range from 12.5 for anhydrochlortetracycline to 17.5 for isochlortetracycline. These values are in an intermediate range that is consistent to those of other drug molecules that have been studied and appear to be typical for drug molecules.^{31,60,61} The Π value for a nonpolar molecule such as cyclohexane is 2.2 kcal/mol, while that for water is 21.6 kcal/mol. The closer is the value of Π to that of water, the more hydrophilic is the compound. Among all of tetracycline compounds isochlortetracycline has the highest solubility in water, and therefore should have a greater mobility, easier bioavailability, and the shortest half-life in soils; this is consistent with it having the largest value of Π in this study. As indicated in an earlier section, isochlortetracycline has been found to be the only transformed compound in this study that has no toxicity to the soil microbial flora.¹⁰ In comparing the Π values in Table 2, it is found that the converse is true for the anhydromers; these have the smallest values of Π, are the least hydrophilic, and have been found to be the most toxic to soil microflora.¹⁰ Table 2 shows that chlortetracycline has an intermediate Π value; it was shown in our previous study to persist in the natural environment for 6 months or longer.⁴⁷ The hydrophilicity and hydrophobicity of the tetracycline compounds are further supported from the calculated log K_{ow} values that are presented in Table 2, with isochlortetracycline being the most hydrophilic (log K_{ow} = -3.6) and anhydrotetracycline being the most hydrophobic (log K_{ow} = 2.2).

As noted earlier σ₊², σ₋², and σ_{tot}² are the positive, negative, and total variances of V_s(r), which reflect the range or variability of V_s(r), emphasizing its surface extrema. From Table 2 it is seen that σ₊² is less than σ₋² for each tetracycline compound, which is typical for most substituted organic molecules.³¹ Among the three parent tetracycline antibiotics, chlortetracycline has the lowest σ₋² and σ_{tot}²; this can be attributed to the large charge capacity of chlorine and its size as discussed earlier. This could result in its greater antibody affinity as compared to tetracycline and oxytetracycline. It is interesting to note from

Table 2 that for all of the tetracycline-epimer pairs, Π and σ_{tot}^2 values show the same decreasing trend in the order tetracycline > epitetracycline, anhydrotetracycline > epianhydrotetracycline, and chlortetracycline > epichlortetracycline. This trend is in good agreement with the increasing antibody cross-reactivity in the order epitetracycline > tetracycline, epianhydrotetracycline > anhydrotetracycline, and epichlortetracycline > chlortetracycline as seen from Table 1. It is observed from Table 2 that σ_+^2 and σ_-^2 show an inverse relationship for tetracycline compounds and their epimers, i.e. when tetracycline compounds epimerize, σ_+^2 decreases and σ_-^2 increases. These observations are in accordance with the fact that the direction of lone pair on the amine nitrogen in the epimers favors easy recognition due to availability of more oriented electronic charge and therefore results in greater antibody binding to the epimers as compared to their parent compounds.

As described earlier, ν indicates the degree of balance between the positive and negative surface potentials. If $\sigma_+^2 = \sigma_-^2$, then ν achieves its maximum possible value of 0.25. Calculated ν values (Table 2) range from 0.13 for oxytetracycline and epitetracycline to 0.22 for chlortetracycline and are indicative of variable degrees of electrostatic balance among tetracycline compounds. Chlortetracycline has the highest electrostatic balance due to the presence of a single chlorine atom; although it is an electron-withdrawing substituent, it distributes its charge over a large volume, as discussed earlier. Our previously made argument that an antibody has a greater cross-reactivity to epimers as compared to its corresponding parent tetracycline compounds is further supported by the fact that all epimers have a low electrostatic balance, due to relatively high σ_-^2 values (as seen from Table 2). The larger values of σ_-^2 for epimers may contribute to greater antibody contact on the molecular surface. On comparing anhydromers, a decrease in electrostatic balance but an increase in σ_-^2 in the order anhydrotetracycline > epianhydrotetracycline explains the increase in antibody cross-reactivity observed for the epimer of anhydrotetracycline. A similar trend is notable for oxytetracycline, which has an intermediate value of σ_-^2 and σ_{tot}^2 (due to negative potential associated with two hydroxyl groups on the top portion of rings B and C) but a low value of electrostatic balance. This results in an intermediate value of antibody cross-reactivity as compared to other tetracycline compounds shown in Table 1.

Molecular Surface Average Local Ionization Energies. Minima of $I_s(\mathbf{r})$ ($I_{s,\text{min}}$) indicate the points on the molecular surface at which the most reactive electrons are found. Figures 3–5, views c and d (Figures 6–11, views c and d in Supporting Information) show the average local ionization energy plotted on the molecular surface of tetracycline compounds. Table 2 shows the lowest atomic $I_{s,\text{min}}$ found on the molecular surface of all tetracycline compounds. It should be noted that values of these minima are greater than the magnitudes of the energies of the highest occupied molecular orbitals because there is always some probability of finding inner, most tightly bound electrons even at these points. As seen from Figures 3–5 views c and d (Figures 6–11 views c and d in Supporting Information) and Table 2 the lowest $I_{s,\text{min}}$ and therefore the most reactive electrons are those associated with lone pairs of the amide nitrogen in all tetracycline compounds. The next lowest $I_{s,\text{min}}$ value for each molecule is the carbon in ring A to which the amide group is bonded. It is notable that the carbons which are *ortho* and *para* to the hydroxyl group on the aromatic ring D are the next most reactive sites in all molecules, except for those containing a chlorine atom. This is consistent with the electron-donating OH group that activates the ring toward *ortho/para*

attack by electrophiles. Table 2 shows higher values of $I_{s,\text{min}}$ for these *ortho/para* aromatic carbons of all chlorine containing tetracycline compounds and Figures 7 (Supporting Information), 8 (Supporting Information), 9 (Supporting Information), and 10 (Supporting Information) show the deactivating nature of the chlorine substituent.

From Table 1 it can be seen that these aromatic carbons do not seem to influence the antibody cross-reactivities to tetracycline compounds as compared to other molecular surface features that were discussed in earlier sections. It is interesting to note that the amide oxygens for epimers of tetracycline and chlortetracycline have lower $I_{s,\text{min}}$ values as compared to those of other tetracycline compounds. The ground-state conformation of these epimers is such that their amide oxygens stick out to the side of the molecule, allowing them to be available for interactions with antibodies. This epimeric configuration of tetracycline and chlortetracycline accounts for greater antibody cross-reactivity to epimers as compared to their parent tetracycline compounds as indicated from experimental ELISA results in Table 1.

Summary

ELISA is the most common format of clinical immunoassay that is highly specific and currently being adapted for environmental analysis to analyze environmental contaminants. ELISA is also used as an essential high-throughput screening tool for a variety of environmental samples with very little sample clean up before subjecting samples to time-consuming and highly rigorous conventional methods of analyses. Antibodies employed in ELISA play a crucial role in its selectivity and specificity to a class of chemical compounds such as tetracycline antibiotics and their metabolites that are formed under natural environmental conditions. For the first time we have characterized parent tetracycline antibiotics and their transformed compounds using molecular surface electrostatic potentials and local average ionization energies and have explained the important role that these molecular surface properties play in influencing the relative affinities of antibody binding to these tetracycline compounds resulting in different cross-reactivities.

Acknowledgment. The authors thankfully acknowledge Dr. Peter Politzer, Department of Chemistry, University of New Orleans, Louisiana for allowing use of the HS95 program written by Dr. Per Sjöberg and Dr. Tore Brinck (cited as ref 50).

Supporting Information Available: Figures 6–11, showing optimized geometry ball and stick models of tetracycline compounds are presented along with electrostatic potential (views a and b) and average local ionization energy (views c and d) mapped on electron density molecular surfaces. This material is available free of charge via the Internet at <http://pubs.acs.org>.

References and Notes

- (1) Ford, T. *Environ. Health Perspect.* **1994**, *102* (Suppl. 12), 45–48.
- (2) Goldberg, B. Antibiotic resistance: Grave threat to human health" online at http://environmentaldefense.org/pubs/Newsletter/1999/Jun/j_antibi.html, 2003.
- (3) Halling-Sørensen, B.; Nielsen, S. N.; Lanzky, F. *Chemosphere* **1998**, *36*, 357–393.
- (4) Herron, P. R.; Toth, I. K. *Soil Biol. Biochem.* **1997**, *30*, 673–677.
- (5) Jørgensen, S. E.; Halling-Sørensen, B. *Chemosphere* **2000**, *40*, 691–699.
- (6) Levy, S. B. *The Antibiotic Paradox. How Miracle Drugs Are Destroying the Miracle*; Plenum Press: New York, 1992.
- (7) Miao, X-S.; Bishay, F.; Chen, M.; Metcalfe, C. D. *Environ. Sci. Technol.* **2004**, *38*, 3533–3541.

- (8) Yang, S.; Cha, J.; Carlson, K. *Rapid Comm. Mass Spec.* **2004**, *18*, 2131–2145.
- (9) Halling-Sørensen, B.; Lykkeberg, A.; Ingerslev, F.; Blackwell, P.; Tjørnelund, J. *Chemosphere* **2003**, *50*, 1331–1342.
- (10) Halling-Sørensen, B.; Sengeløv, G.; Tjørnelund, J. *Arch. Environ. Contam. Toxicol.* **2002**, *42*, 263–271.
- (11) Koplín, D. W.; Furlong, E. T.; Meyer, M. T.; Thurman, E. M. *Environ. Sci. Technol.* **2002**, *36*, 1202–1211.
- (12) Engvall, E.; Perlman, P. *Immunochem.* **1971**, *8*, 871–874.
- (13) Lequin, R. *Clin. Chem.* **2005**, *51*, 2415–2418.
- (14) Scrocco, E.; Tomasi, J. *Top. Curr. Chem.* **1973**, *42*, 95–100.
- (15) Politzer, P.; Truhlar, D. G., Eds. *Chemical Applications of Atomic and Molecular Electrostatic Potentials*; Plenum: New York, 1981.
- (16) Murray, J. S.; Politzer, P. *J. Mol. Struct. (THEOCHEM)* **1998**, *425*, 107–111.
- (17) Feynman, R. P. *Phys. Rev.* **1939**, *56*, 340–348.
- (18) Hirschfelder, J. O.; Curtiss, C. F.; Bird, R. B. *Molecular Theory of Gases and Liquids*; Wiley: New York, 1954.
- (19) Hirschfelder, J. O. In *Molecular Forces*; North-Holland: Amsterdam, 1967; Sect. 4, pp 1–61.
- (20) Hunt, K. L. *J. Chem. Phys.* **1990**, *92*, 1180–1185.
- (21) Naray-Szabo, G.; Ferenczy, G. *Chem. Rev.* **1995**, *95*, 829–834.
- (22) Margenau, H.; Murphy, G. M. *The Mathematics of Physics and Chemistry*, 2nd. ed.; Van Nostrand: Princeton, NJ, 1956.
- (23) Hohenberg, P.; Kohn, W. *Phys. Rev. B* **1964**, *136*, 864–870.
- (24) Weinstein, H.; Politzer, P.; Srebrenik, S. *Theor. Chim. Acta.* **1975**, *38*, 159–166.
- (25) Bonaccorsi, R.; Scrocco, E.; Tomasi, J. *J. Chem. Phys.* **1970**, *52*, 5270–5276.
- (26) Bonaccorsi, R.; Scrocco, E.; Tomasi, J. *Theor. Chim. Acta* **1971**, *21*, 17–21.
- (27) Bonaccorsi, R.; Pullman, A.; Scrocco, E.; Tomasi, J. *Chem. Phys. Lett.* **1972**, *12*, 622–628.
- (28) Berthier, G.; Bonaccorsi, R.; Scrocco, E.; Tomasi, J. *Theor. Chim. Acta* **1972**, *26*, 101–104.
- (29) Bonaccorsi, R.; Pullman, A.; Scrocco, E.; Tomasi, J. *Theor. Chim. Acta* **1972**, *24*, 51–55.
- (30) Yuko, T.; Kinoshita, K.; Nakamura, H. *Proc. Struct. Funct. Bioinform.* **2004**, *55*, 885–894.
- (31) Murray, J. S.; Abu-Awwad, F.; Politzer, P.; Wilson, L. C.; Troupin, A. S.; Wall, R. E. *Int. J. Quantum Chem.* **1998**, *70*, 1137–1143.
- (32) Hagelin, H.; Brinck, T.; Berthelot, M.; Murray, J. S.; Politzer, P. *Can. J. Chem.* **1995**, *73*, 483–490.
- (33) Bader, R. F. W.; Carroll, M. T.; Cheeseman, J. R.; Chang, C. *J. Am. Chem. Soc.* **1987**, *109*, 7968–7978.
- (34) Politzer, P.; Murray, J. S. In *Reviews in Computational Chemistry*; Lipkowitz, K. B., Boyd, D. B., Eds., VCH: New York, 1991; Vol. 2.
- (35) Murray, J. S.; Politzer, P. In *Quantitative Treatments of Solute/Solvent Interactions*, Murray, J. S., Politzer, P., Eds., Elsevier: Amsterdam, 1994.
- (36) Murray, J. S.; Brinck, T.; Lane, P.; Paulsen, K.; Politzer, P. *J. Mol. Struct. (THEOCHEM)* **1994**, *307*, 55–61.
- (37) Fricke, B. *J. Chem. Phys.* **1986**, *84*, 862–868.
- (38) Politzer, P. *J. Chem. Phys.* **1987**, *86*, 1072–1077.
- (39) Berkowitz, M.; Parr, R. G. *J. Chem. Phys.* **1988**, *88*, 2554–2560.
- (40) Parr, R. G.; Yang, W. *Density-Functional Theory of Atoms and Molecules*; Oxford University Press: New York, 1989.
- (41) Politzer, P.; Murray, J. S.; Grice, M. E.; Brinck, T.; Ranganathan, S. *J. Chem. Phys.* **1991**, *95*, 6699–6710.
- (42) Parr, R. G.; Yang, W. *Annu. Rev. Phys. Chem.* **1995**, *46*, 701–708.
- (43) Murray, J. S.; Politzer, P. In *Theoretical Organic Chemistry*; Parkanyi, C., Ed.; Elsevier: Amsterdam, 1998.
- (44) Sjöberg, P.; Politzer, P. *J. Phys. Chem.* **1990**, *94*, 3959.
- (45) Sjöberg, P.; Murray, J. S.; Brinck, T.; Politzer, P. *Can. J. Chem.* **1990**, *68*, 1440.
- (46) Murray, J. S.; Brinck, T.; Politzer, P. *J. Mol. Struct. (THEOCHEM)* **1992**, *255*, 271.
- (47) Kulshrestha P., Giese, R. F. Wood, T. D. Residue analysis of tetracycline antibiotics in soil fertilized with manure and wastewater using ELISA and LC-MS. *Anal. Chim. Acta*, submitted.
- (48) Frisch, M. J.; Trucks, G. W.; Schlegel, H. B.; Scuseria, G. E.; Robb, M. A.; Cheeseman, J. R.; Zakrzewski, V. G.; Montgomery, J. A.; Stratmann, R. E.; Burant, J. C.; Dapprich, S.; Millam, J. M.; Daniels, A. D.; Kudin, K. N.; Strain, M. C.; Farkas, O.; Tomasi, J.; Barone, V.; Cossi, M.; Cammi, R.; Mennucci, B.; Pomelli, C.; Adamo, C.; Clifford, S.; Ochterski, J.; Petersson, G.; Ayala, P. Y.; Cui, Q.; Morokuma, K.; Malick, D. K.; Rabuck, A. D.; Raghavachari, K.; Foresman, J. B.; Cioslowski, J.; Ortiz, J. V.; Stefanov, B. B.; Liu, G.; Liashenko, A.; Piskorz, P.; Komaromi, I.; Gomperts, R.; Martin, R. L.; Fox, D. J.; Keith, T.; Al-Laham, M. A.; Peng, C. Y.; Nanayakkara, A.; Gonzalez, C.; Challacombe, M.; Gill, P. M. W.; Johnson, B. G.; Chen, W.; Wong, M. W.; Andres, J. L.; Head-Gordon, M.; Replogle, E. S.; Pople, J. A. *Gaussian 98, Revision A.5*, Gaussian: Pittsburgh, PA, 1998.
- (49) Breneman, C. M.; Sundling, C. M.; Sukumar, N.; Shen, L.; Katt, W. P.; Embrechts, M. J. *J. Comput. Aid. Mol. Des.* **2003**, *17*, 231–240.
- (50) Sjöberg, P., Brinck, T. *MOLSURF* is marketed by Quemist AB, Hertig Karls Alle 29, S-69141 Karlskoga, Sweden, 1995.
- (51) Doerschuk, A. P.; Bitler, B. A.; McCormik, J. R. D. *J. Am. Chem. Soc.* **1955**, *77*, 4687–4692.
- (52) McCormik, J. R. D.; Fox, S. M.; Smith, L. L.; Bitler, B. A. *J. Am. Chem. Soc.* **1957**, *79*, 2849–2851.
- (53) Breen, K.; Schenker, S.; Heimberg, M. *Biochim. Biophys. Acta* **1972**, *270*, 74–80.
- (54) Chopra, I.; Hawkey, P. M.; Hinton, M. *J. Antimicrob. Chemother.* **1992**, *29*, 245–277.
- (55) Mitscher, L. A. *The chemistry of tetracycline antibiotics. Medicinal research series 9*, Marcel Dekker, New York, 1978.
- (56) Blackwood, R. K.; English, A. R. *Adv. Appl. Microbiol.* **1970**, *13*, 237–266.
- (57) Politzer, P.; Concha, M. C.; Murray, J. S. *Int. J. Quantum Chem.* **2000**, *80*, 184–192.
- (58) Murray, J. S.; Peralta-Inga, Z.; Politzer, P. *Int. J. Quantum Chem.* **1999**, *75*, 267–274.
- (59) Hussein, W.; Walker, C. G.; Peralta-Inga, Z.; Murray, J. S. *Int. J. Quantum Chem.* **2001**, *82*, 160–169.
- (60) Brinck, T.; Jin, P.; Ma, Y.; Murray, J. S.; Politzer, P. *J. Mol. Mod.* **2003**, *9*, 77–85.
- (61) Gonzalez, O. G.; Murray, J. S.; Peralta-Inga, Z.; Politzer, P. *Int. J. Quantum Chem.* **2001**, *83*, 115–121.